SLOPE STABLITY ANALYSIS REGARDING RAINFALL-INDUCED LANDSLIDES BY COUPLING SATURATED-UNSATURATED SEEPAGE ANALYSIS AND RIGID PLASTIC FINITE ELEMENT METHOD

Yu. Ando [1], Kentaro. Suda [2], Shinji. Konishi [3] and Hirokazu. Akagi [4]

ABSTRACT: This paper presents a new slope stability analysis regarding rainfall-induced landslides by coupling a saturated-unsaturated seepage analysis and a rigid plastic finite element method (RP-FEM). Currently, a more valid and reliable disaster prevention system detecting the risk of slope instability due to sudden intense rainfall is required in Japan. However, conventional slope stability methods often fail to predict this new type of landslides. Therefore, the aim of this study is to propose the new slope stability analysis method in the context of rainfall infiltration. This method introduces the effect of seepage force, an increase of unit weight and a reduction of apparent cohesion due to the change in soil suction to obtain the slope stability load factors and collapse mechanisms. Consequently, this method can provide the relatively accurate and valid analysis results, which can be well compared with experimental data. Moreover, it is ascertained that this method can evaluate the different type of slope failure mechanisms: an initial small failure at the toe of the slope caused by the seepage forces and a large-scale failure due to the degradation of the soil apparent cohesion

Keywords: slope stability, numerical analysis, rainfall, infiltration

1. INTRODUCTION

In recent years, landslides caused by heavy rain are reported in various parts of Japan. There have been reports of more than 1000 failure cases since 2009 to 2011 and 1043 cases only in year 2014. Embankment and slope failure due to rainfall are mainly because of a reduction of the shear strength with decrease of suction, increase in soil self weight, and the change of the ground water level by the infiltration of the rain water.

This study aims to propose a new analytical method which can evaluate the slope stability by considering the failure factors: an increase in soil self weight by the infiltration of the water, a decrease in soil apparent cohesion due to the drop of soil suction and an influence of water seepage pressure.

In this study, a seepage analysis has been done to obtain ground water and pore water pressure distribution in slope and investigate that destabilization factors of slope due to the infiltration of the rain. These factors are introduced into the Rigid Plastic FEM (RP-FEM).

Slope stability analysis has been performed based on the plasticity theory and large deformation problems have been solved in detail at the slope collapse. Rigid-plastic model can be used to demonstrate the plastic flow behavior at limit state. Moreover, in RP-FEM it is not necessary to assume a slip surface line for a limit equilibrium method, and it only requires a few parameters such as cohesion, internal friction angle, and water pressure. Three destabilization factors mentioned in the previous section can also be taken into account.

Methodology flowchart in this study is shown in Fig.1. In order to confirm the validity of this analysis, numerical simulation results are compared with soil slope model test data by Kitamura et al., 2007.
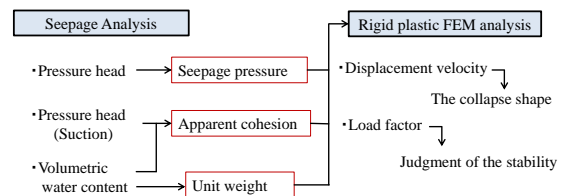

Fig. 1. Methodology flowchart in this study

[1] Student, Waseda University, 3-4-1 Okubo, Shinjuku-ku, Tokyo, JAPAN
[2] Student, Waseda University, 3-4-1 Okubo, Shinjuku-ku, Tokyo, JAPAN
[3] Researcher, Tokyo Metro Co., Ltd., 3-19-6 Higashiueno, Daito-ku, Tokyo, JAPAN
[4] Professor, Waseda University, 3-4-1 Okubo, Shinjuku-ku, Tokyo, JAPAN

2. INTRODUCTION TO THE SLOPE DESTAB-LIZATION FACTORS

2.1 Pressure head and seepage pressure

One of the major reasons for slope failures due to rainfall is the effect of seepage forces. In order to introduce the effect of water seepage forces in RP-FEM, seepage forces obtained by the pressure head distribution from a seepage analysis are converted into equivalent nodal forces. Eq. (1) indicates the relationship between the pressure head and the seepage force at any points in the soil elements. Eq. (2) is the Gaussian integrated to obtain the equivalent nodal force in each element.

$$\{\gamma_w \cdot i\} = \gamma_w \cdot \left\{ \begin{array}{c} -\dfrac{\partial h}{\partial x} \\ -\dfrac{\partial h}{\partial y} \end{array} \right\} = \gamma_w \cdot \left\{ \begin{array}{c} -\sum_{j=1}^{n} \dfrac{\partial N_j}{\partial x} h_j \\ -\sum_{j=1}^{n} \dfrac{\partial N_j}{\partial y} h_j \end{array} \right\} \quad (1)$$

$$\begin{cases} f_x = -\int_{\Omega} N^T \gamma_w \dfrac{\partial h}{\partial x} d\Omega \\ f_y = -\int_{\Omega} N^T \gamma_w \dfrac{\partial h}{\partial y} d\Omega \end{cases} \quad (2)$$

where γ_w is a unit weight of water, i is a hydraulic gradient, h is a pressure head, N is a shape function, n is the number of nodes, f_x and f_y are equivalent nodal forces, and Ω is the integral regime

2.2 Relation among soil suction, saturation and the apparent cohesion

The apparent cohesion is calculated by using the relation between Ψ: suction and θ: water content, as shown by Karube[2]. The effective stress of unsaturated soil is given by Eq. (3), in which soil suction is incorporated into the relation between total stress and effective stress, presented by Bishop et al., 1960.

$$\sigma' = (\sigma - u_w) + \chi \cdot (u_a - u_w) \quad (3)$$

where σ is total stress, u_a is an air pressure, u_w is a pore water pressure, (u_a-u_w) is a suction and χ is an empirical constant. Eq. (3) is substitute into Mohr-Columb failure criterion, and by assuming a constant internal friction angle, soil internal friction angle ϕ and cohesion c are given as bellow.

$$\begin{cases} \phi = \phi' \\ c = c' + \chi \cdot (u_a - u_w) \cdot \tan \phi' \end{cases} \quad (4)$$

where c is an apparent cohesion, c' is a cohesion at saturation, ϕ is an internal friction angle, ϕ' is an effective internal angle. Karube[2] has empirically obtained the constant χ : experiment constant as indicated in Eq. (4).

$$\chi = \frac{S_r - S_{r0}}{100 - S_{r0}} \quad (5)$$

where S_r is the degree of saturation, S_{r0} is the minimum saturation. By substitution of Eq. (5) into Eq. (4), cohesion and internal friction angle of unsaturated soil can be represented as follows.

$$\begin{cases} \phi = \phi' \\ c = c' + \dfrac{S_r - S_{r0}}{100 - S_{r0}} \cdot (u_a - u_w) \cdot \tan \phi' \end{cases} \quad (6)$$

Van Genuchten model determines the relation between the degree of saturation (S_e) and soil suction as

$$Se = \left\{ 1 + \left(-\alpha \cdot \varphi_m \right)^n \right\}^{-m} \quad (7)$$

where S_e is the effective saturation, α, m and n are non-dimensional parameters.

3. OUTLINE OF THE EXPERIMENTAL STUDY

3.1 Soil slope model test

Systematic experimental study has been carried out by Kitamura et al., 2007. Fig. 2 indicates the schematic diagram of soil slope model test, where water is injected from the bottom, back and top part of the slope respectively. Seepage and failure behavior are observed during water infiltration by installed tensiometers (No.1~15) and piezometers at the bottom observing pore water pressures. For simplicity, the test condition for infiltration from the bottom is named as case 1, injection from the back named as case 2, and injection from the top named as case 3, respectively.
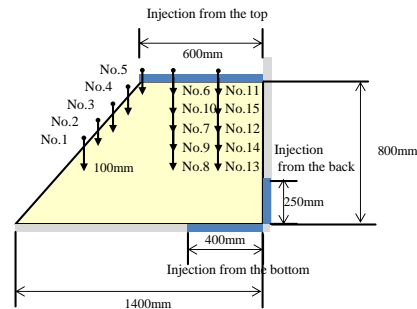

Fig. 2. Soil slope model test

3.2 Status of infiltration of water into model test

There are three water infiltration cases into the model. In case 1, constant water head of h=25cm is introduced to the bottom of model as shown in Fig. 2. After the phreatic line reached the toe of the slope, partial collapse happened at the toe after 120min, and then collapse zone gradually expanded (progressive failure). Large-scale failure occurred after 260min.

In case 2, constant water head (h=25cm) is given at the back of slope as shown in Fig. 2. In this case, small failure occurred after 160 min, and after this initial collapse, collapsed zone expanded at some extent, however, large-scale failure did not happen.

In case 3, the constant flow rate (4.0 liter/min) is given from the top of the soil slope. In this case, water infiltrated and reached at the bottom of tank, and then flowed into the toe while forming water table in the slope. The collapse at the toe happened at 110 min, and the large scale collapse happened at 115 min.

4. SEEPAGE ANALYSIS

4.1 Numerical analysis model and soil properties

Table.1 indicates the soil properties used in the analysis. The experimental values obtained by model test have been used, and the remainder is assumed by using the general soil properties. Fig. 3 shows the model used for analysis. It consists of 1881 rectangular elements. This model is used for the test conditions of case 1,2 and 3.

4.2 Analysis case details

For the test case 1, the constant water head is given at the bottom of the soil slope as shown in Fig.3. Initial pressure head at each element is constant and is -800 mm and the constant water head at the boundary is fixed at 250 mm. For the test case 2, the constant water head is given at the back of the soil slope shown in Fig.3 Initial pressure head in each element is constant and is -700 mm and constant water level at the boundary is fixed at 250 mm. For test case 3, constant infiltration at the boundary is given at top of the soil slope as shown in Fig. 3. Initial pressure head in each element is constant at -800mm and flow rate at the boundary is fixed at 0.37mm/node. Figs. 4, 5, and 6 indicate unsaturated soil hydraulic properties for test cases 1, 2, and 3 respectively. Unsaturated soil hydraulic properties are determined by fitting analysis values with experimental data and the theoretical line by Van Genuchten model.

Table1. 1. Soil properties

| Condition	1	2	3	
Water Unit waight γ_w (kN/m³)	9.81	9.81	9.81	General
Soil particle unit waight γ_s (kN/m³)	24.04	24.00	24.00	
Dry weight of the ground γ_d (kN/m³)	9.35	9.72	9.34	
Void ratio e	1.57	1.47	1.57	Experiment
Internal friction angle ϕ (°)	38.0	38.0	38.0	
Saturation permeability k (m/s)	5.75×10^{-5}	1.87×10^{-5}	4.83×10^{-5}	
Ratio retention coefficient S_S (1/mm)	1.00×10^{-5}	1.00×10^{-5}	1.00×10^{-5}	Estimate
Saturation cohesion c (kN/m²)	0.0	0.0	0.0	
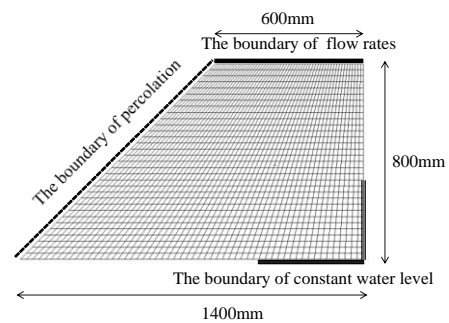
Fig. 3. Analysis model
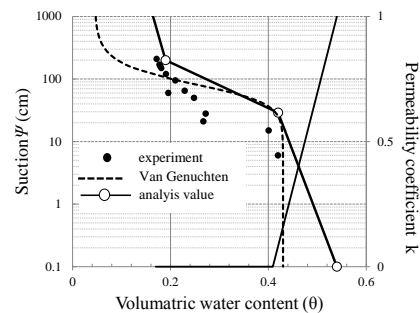
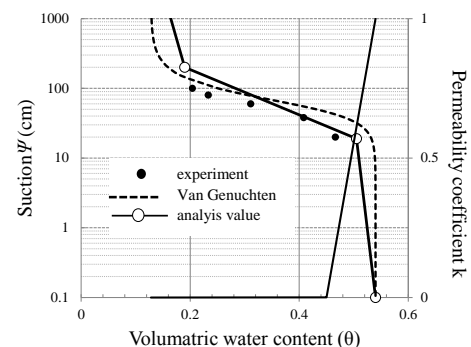Fig. 4. Unsaturated soil hydraulic properties 1

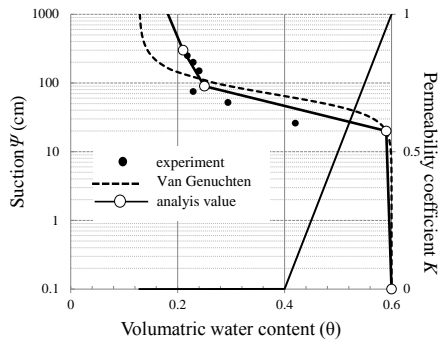Fig. 5. Unsaturated soil hydraulic properties 2

Fig. 6. Unsaturated soil hydraulic properties 3

4.3 Analysis results

The changes of pore water pressure in soil are measured by the tensiometers in Fig. 2. Fig. 7 indicates the comparison between experimental data (a) and analyzed results (b) in test case 1. Fig. 8 and Fig. 9 are the comparisons of the experimental data with analyzed results for test case 2 and 3 respectively. Based on Figs. 7-9, it can be seen that seepage analysis can successfully reproduce the water infiltration into the soil and also the change in pore water pressure in each test case.
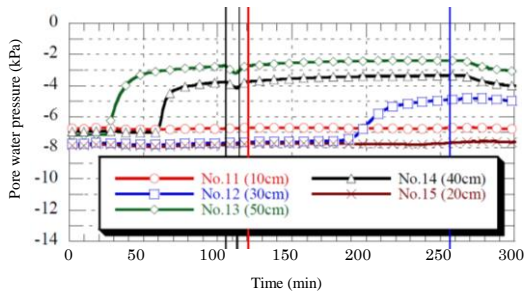
(a) Measured pore water pressure
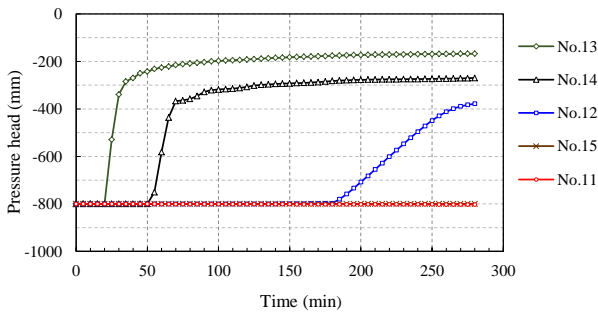
(b) Analyzed pressure head
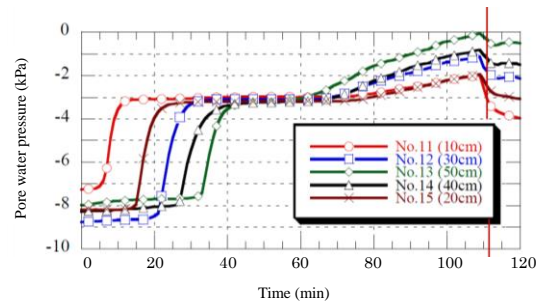Fig. 7.Comparison of experiment with analysis case 1
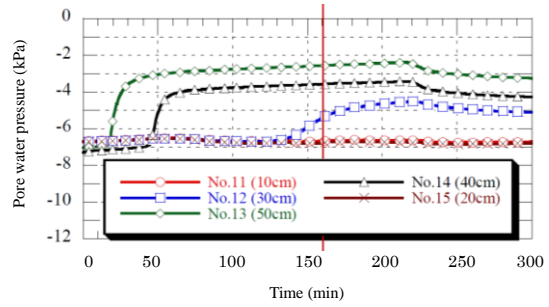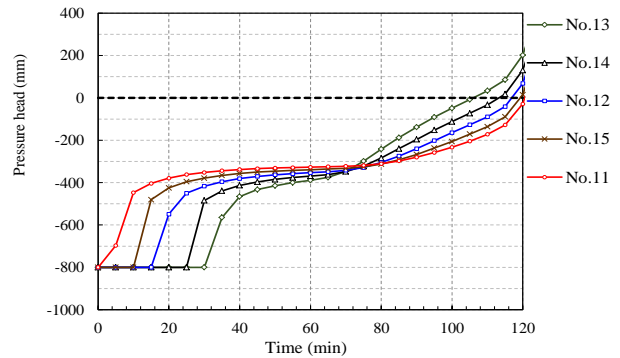

(a) Measured pore water pressure
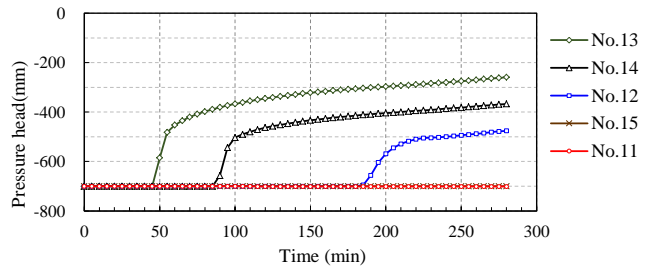
(b) Analyzed pressure head
Fig. 8.Comparison of experiment with analysis case 2

(a) Measured pore water pressure

(b) Analyzed pressure head
Fig. 9.Comparison of experiment with analysis case 3

5. RIGID PLASTIC FE SLOPE STABILITY ANALYSIS

5.1 Rigid plastic FE analysis

Rigid plastic FE analysis is the method to obtain the stress distribution, the displacement velocity and the load factor μ when collapse occurs. It employs the upper bound theorem to solve the equilibrium of stress and the compatibility condition of strain velocity. Time dependent seepage force, increased soil unit weight and soil apparent cohesion reduced by water infiltration has been introduced into RP-FEM analysis. The value of soil slope load factor μ has been obtained to satisfy the force equilibrium of the whole FE model at the specified time period. Yielding condition is defined by the Mohr-Couomb failure criterion and the plastic flow is given by the Drucker-Prager yield criterion. Load factor μ is equivalent to a safety factor of slope stability. Therefore, load factor $\mu=1$ indicates ordinary gravitational field, while $\mu \gueq 1$ indicates that the soil slope is stable and $\mu<1$ indicates that the soil slope is unstable.

5.2 Analysis model and soil property

The analysis model and soil properties used in the RP-FEM analysis are the same as in the seepage analysis.

5.3 Analysis method

Displacement boundary conditions are given as follows: the bottom nodes have been fixed vertically and horizontally and the side nodes have been fixed horizontally. Load factors of slope stability analysis have been computed by introducing data of seepage force, an apparent cohesion and a unit weight into rigid plastic FEM.

5.4 Analysis results

Fig.10 indicates the time-dependent change of load factor μ with infiltration of water from the bottom (test case 1). It can be seen that the load factor μ reaches at the value of 0.33 at 100 min and 0.02 at 200 min which indicates that the slope collapsed twice. These collapses correspond to the initial failure at the toe at 120 min and large scale failure at 260 min in the experiment. In fact, the factor of safety has already become smaller than $\mu =1$ at 75 min in the numerical simulation result. In terms of the time periods where the factor has become the minimum, the seepage pressure acts on the toe of the slope at 100 min (Fig. 11), and the majority part of the slope loses its apparent cohesion at 200 min (Fig. 12).
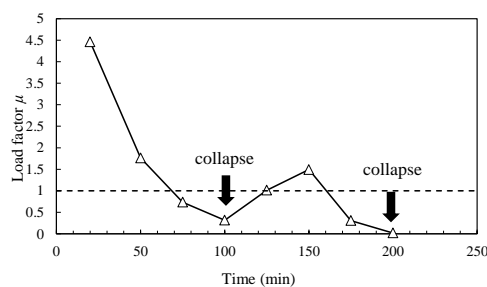

Fig. 10. Time dependent variation of load factor μ in case 1
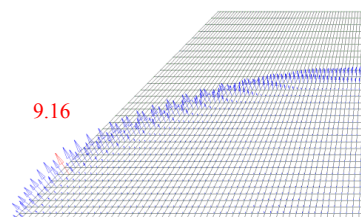

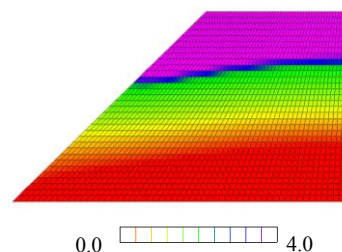Fig. 11. Distribution of seepage force at 100min in case 1 ($\times 10^{-3}$N)

Fig. 12. Distribution of cohesion at 200min in case 1 (kN/m^2)

Fig. 13 indicates the time-dependent change of load factor μ by infiltration of water from the back (test case 2). It can be seen, that the load factor μ reaches at the value of 0.97 at 170 min in Fig. 13. Also, this collapses correspond to failure at the toe at 160 min in the experiment. In terms of the time period where the factor has become the minimum, the seepage pressure acts on the toe of the slope at 170min (Fig.14), and the majority part of the slope loses its apparent cohesion at 170 min (Fig. 15).

Fig.16 indicates the time-dependent change of load factor μ by injection of water from the top (test case 3). It can be seen that the load factor μ reaches at the minimum of 0.81 at 110 min and 0.22 at 120 min in Fig.16. Also, these collapses correspond to the initial failure at the toe at 110 min and large scale failure at 115 min obtained in the experiment. In terms of the time period where the load factor has become the minimum, the seepage pressure acted on the toe of the slope at 110 min (Fig. 17), and the ma-

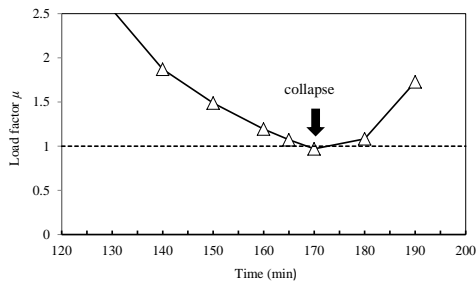jority part of the slope lost its apparent cohesion at 120 min (Fig. 18)

Fig. 13. Time dependent variation of load factor μ in case 2
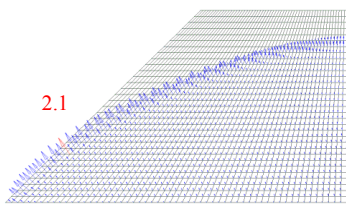

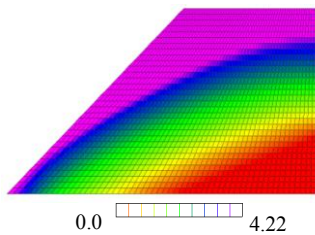Fig. 14. Distribution of seepage force at 170min in case 2 ($\times 10^{-3}$N)

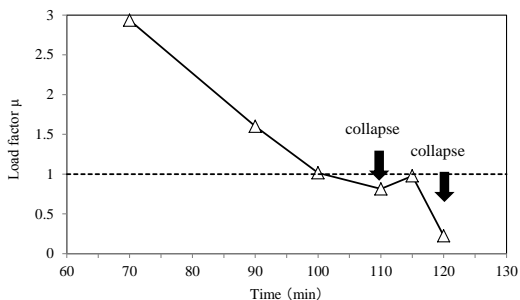Fig. 15. Distribution of cohesion at 170min in case 2 (kN/m^2)

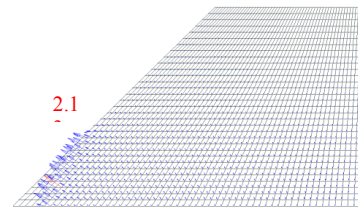Fig.16. Time dependent variation of load factor μ in case 3

Fig.17. Distribution of seepage force of 110min in case 3 ($\times 10^{-3}$N)
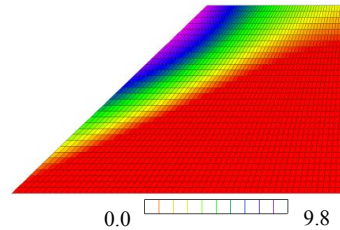

Fig. 18. Distribution of cohesion at 120min in case 3 (kN/m^2)

6. CONCLUSIONS

In this study, the stability of slope in the experiment conducted by Kitamura et al., 2007 was evaluated by using slope stability analysis by coupling seepage analysis and rigid plastic FEM. The conclusions obtained from this study are summarized as follows.

1) The distribution of soil seepage forces, unit weight, and soil apparent cohesion at failure was successfully simulated by the seepage analysis.

2) The validity of this slope stability analysis was ascertained by the result that the time of failure in analysis corresponds to the time of failure obtained in the experiment. In addition, the destabilization factors (seepage forces, unit weight, and apparent cohesion) have been demonstrated to influence on the stability analysis by RP-FEM.

3) By using the proposed method, the progressive failure (the initial failure at the toe of the slope and the gradual propagation of the failure area) can also be explained based on the time-dependent change of load factors.

REFERENCES

1) Karube, D., Kato, S., Hamada, K., Honda, M. (1996). "The relationship between the mechanical behavior and the state porewater in unsaturated soil", Journal of JSCE, No.554, pp83-92 (in Japanese)
2) Kitamura, R., Sako, K., Kato, S., Mizushima, T. (2005). "Soil tank test on seepage and failure behaviors of Shirasu the slope during rainfall", Journal of JGS, Vol.2, No 3, pp149-168 (in Japanese)
3) Konishi, S., Nakayama, T., Tamura, T., Toyota, H., Matsunaga, T., Iura, T. (2013). "Evaluation of tunnel face stability affected by ground water and varying cohesion of sandy layer due to degree of saturation", Journal of JSCE, Vol.69, No. 1, pp1-9 (in Japanese)